Int. J. Electrochem. Sci., 11 **(2016)** 2799 - 2824

International Journal of ELECTROCHEMICAL SCIENCE
www.electrochemsci.org

Electrochemical Methods for Study of Influence of Selenium Nanoparticles on Antioxidant Status of Rats

Pavel Horky[1], Branislav Ruttkay-Nedecky[2,3], Lukas Nejdl[2,4], Lukas Richtera[3,4], Natalia Cernei[2,3], Miroslav Pohanka[4], Pavel Kopel[2,3], Jiri Skladanka[1], Pavlina Hloucalova[1], Petr Slama[5], Pavel Nevrkla[6], Veronika Mlejnkova[1], Iva Klusonova[1], Rene Kizek[2,3] and Vojtech Adam[2,3]*

[1] Department of Animal Nutrition and Forage Production, Faculty of Agronomy, Mendel University in Brno, Zemedelska 1, CZ-613 00 Brno, Czech Republic, European Union
[2]Central European Institute of Technology, Brno University of Technology, Technicka 3058/10, CZ-616 00 Brno, Czech Republic, European Union
[3]Department of Chemistry and Biochemistry, Mendel University in Brno, Zemedelska 1, CZ-613 00 Brno, Czech Republic, European Union
[4]Department of Geology and Pedology, Mendel University in Brno, Zemedelska 1, CZ-613 00 Brno, Czech Republic, European Union
[5]Department of Animal Morphology, Physiology and Genetics, Faculty of Agronomy, Mendel University in Brno, Brno, Czech Republic, European Union
[6] Department of Animal Breeding, Faculty of Agronomy, Mendel University in Brno, Zemedelska 1, CZ-613 00 Brno, Czech Republic, European Union
[*]E-mail: vojtech.adam@mendelu.cz

Received: 8 January 2016 / *Accepted:* 27 January 2016 / *Published:* 1 March 2016

The aim of the experiment was to determine the effect of selenium nanoparticles (SeN) and selenium nanoparticles bound with glucose (SeN-GLU) on the antioxidant status of rats. The rats were fed with two defined forms of selenium nanoparticles for ten days. The first experimental group (n=6) was dosed with SeN solution (0.06 mg of Se per kg of body weight / day). The second experimental group (n=6) was dosed with SeN-GLU (0.06 mg of Se and 0.3 mg of glucose per kg of body weight / day). In both experimental groups, the antioxidant activity was decreased in rat plasma and increased in liver, when measured using the both free radicals (FR) and Ferric Reducing Antioxidant Power (FRAP) method. Electrochemical technique (differential pulse voltammetry-DPV) was applied to analyze the content of metallothionein (MT) and heavy metals. The reduced and oxidized forms of glutathione were analyzed by high performance liquid chromatography with electrochemical detection (HPLC-ED). In the analysis of whole blood, a significant increase of reduced glutathione (GSH) by 41% ($P < 0.05$) was observed in the SeN-GLU group compared with the control goup. Higher levels of GSH were also observed in the SeN group by 12%, but without any statistical significance. On the other hand, a smaller increase in oxidized glutathione (GSSG) by 22% ($P < 0.05$) was observed for the SeN-GLU group and an insignificant decrease by 13% was recorded for the SeN group which implies increased GSH/GSSG ratio and higher antioxidant activity for both SeN-GLU and SeN groups in the whole blood. In the assessing of GSH in erythrocytes, a linear increase was observed for each group.

An increase by 14% in the SeN group and a significant increase by 19% ($P < 0.05$) in the SeN-GLU group of rats was recorded. The amount of GSSG was the highest in the SeN group (an increase by 21%). In the liver, decrease in both forms of glutathione was observed. MT values were significantly higher in erythrocytes, plasma and liver in the groups with addition of SeN and SeN-GLU, which again implies higher antioxidant activity. The levels of zinc and copper were not significantly changed in the plasma or in the liver. From these results, it is apparent that SeN and SeN-GLU may be considered as an alternative source of selenium for improving of antioxidant status of the animal organism, which is characterized by high usability.

Keywords: selenium nanoparticles; antioxidant; rat; animal nutrition; selenium; supplementation

1. INTRODUCTION

Selenium plays an important role in the terms of the antioxidant mechanism and the elimination of free radicals [1,2]. Free radicals are the part of the physiological processes in the body [3,4]. If there is the excessive production of reactive oxygen species, the oxidative stress can occur leading to various diseases such as cancer [5-9]. Selenium is required for the proper activity of a group of enzymes called glutathione peroxidases (GPx). These enzymes play a key role in the body's detoxification system and they also provide protection against the oxidative stress [10]. The most common sources of selenium include sodium selenite and selenium amino acids (such as selenocysteine, selenocystine and mainly with seleno-methionine which is the major dietary form). Nowadays, researchers try to develop new forms of selenium serving as an alternative source for selenium supplement for the animal body. Selenium deficiency results in a higher rate of lipid peroxidation, damage of membrane structures, impaired reproduction, rapid aging of the organism [11-13]. Therefore, the selenium supplement is recommended to the diet not only for humans but also for livestock [14-16].

The studies have shown that the organic forms of selenium are more digestible, more accessible to the organism and more biologically active than the inorganic forms [16-18]. Furthermore, selenium has been investigated for various medical applications such as anticancer applications. Selenium as a dietary supplement has been demonstrated to reduce the risks of various types of cancers including prostate cancer, lung cancer, esophageal and gastric-cardiac cancers [19,20]. Selenium, enriched with probiotics, has been shown to strongly inhibit the growth of pathogenic *Escherichia coli in vivo* and *in vitro* [21]. Another study by Zhou *et al*. demonstrated that the selenium nanoparticles increase the formation of muscle more than the organic selenium [22]. Recently, the materials of nanometric size have attracted the considerable attention because the nanoparticles can overcome the existing mechanisms and may serve as nanotransporters. Nanoparticles can be variously modified and becoming active and thus be the ideal medium for the targeted drug delivery as well as for nutrients in the body [23]. Nanoparticles possess the increased surface areas and therefore have increased interactions with biological targets (such as bacteria) compared with conventional microparticles [24]. Selenium nanoparticles are attracting increasing attention due to their excellent biological activities and a low toxicity [25,26]. Many studies showed that selenium nanoparticles exhibited novel *in vitro* and *in vivo* antioxidant activities through the activation of selenoenzymes [27-29]. However, so far

very little information about the antiproliferative activity of selenium nanoparticles and the underlying mechanisms could be obtained.

Electrochemical methods provide high potential for investigation of antioxidant compounds such as glutathione, metallothionein (MT) and also for detection of heavy metals. Different types of electrodes can be used for the assay purposes. The devices can be stationary [30-36] or flowthrough [37-42] and based on cyclic or differential pulse voltammetry (DPV) as well as potentiostatic analysis.

The aim of the experiment was to determine whether new forms of selenium, based on nanotechnology, can increase the antioxidant status of rats. For this purpose, electrochemical technique (DPV) was applied to analyze the content of MT and heavy metals. Further, for analysis of the reduced and oxidized forms of glutathione (GSH, GSSG) flowthrough electrochemical method high performance liquid chromatography with electrochemical detection (HPLC-ED) was used.

2. EXPERIMENTAL PART

2.1. Animals

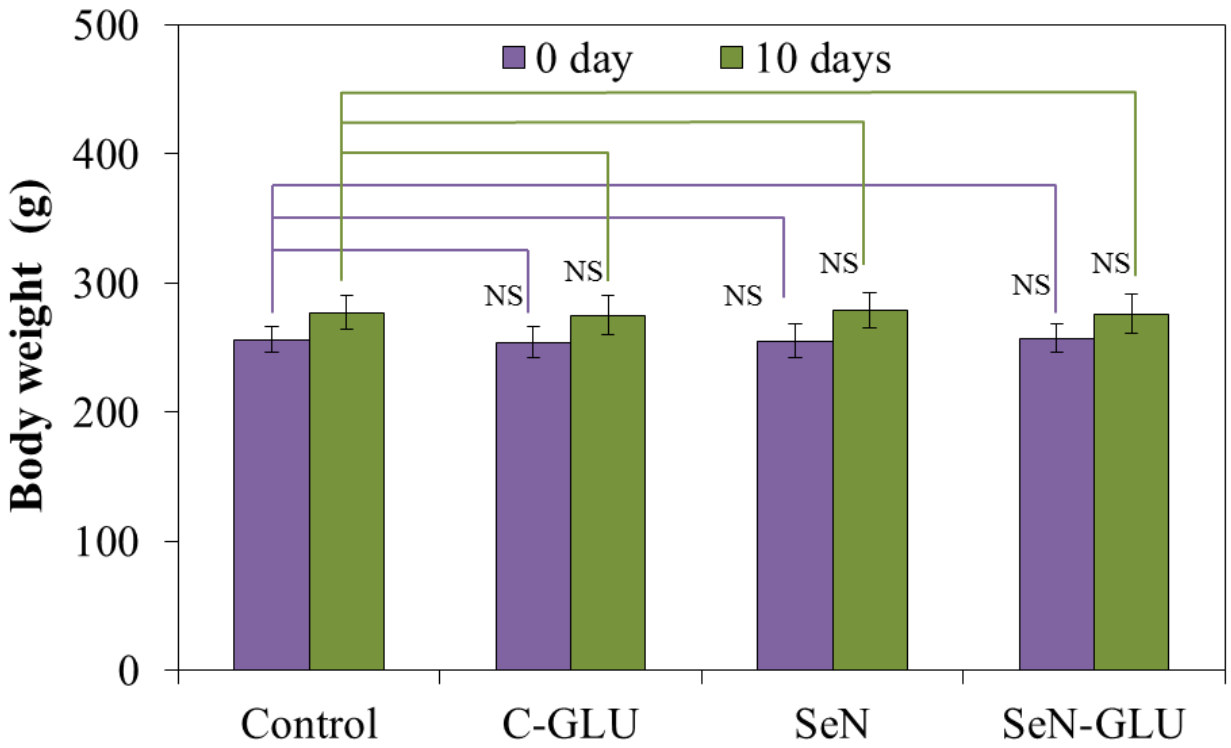

Figure 1. The influence of different forms of selenium on the weight of the rats during the ten-day experiment. All data represent mean ± s d. from 5 measurements, NS, not significant, * $P < 0.05$. Other experimental details see in Material and Methods section.

The experiment was conducted at the experimental facility of the Department of Animal Nutrition and Forage Production, MENDELU (in accordance with the Law on protection of animals

against cruelty No. 246/1992). In the laboratory, the climatic conditions were monitored, which were primarily limited by the temperature measured by "Data Logger with 3120" and maintained between 23 °C ± 1°C. Furthermore, the same device was used for the monitoring of constant humidity. The air conditioning unit was set at a level of 60 %. The photoperiod was artificially controlled by the following scheme: for 12 h per day and for 12 h per night and with the maximum intensity of 200 lux. Male rats of *Wistar albino* outbreed strain were used as an experimental model for this experiment. The average weight of rats was 256 ± 5 g at the beginning of the experiment. The experimental observation lasted for 10 days. The average weight of rats in the tenth day of experiment was 276 ± 5 g (Fig.1). The rats were housed in the plastic cages with shelves. The animals had the access to food and water *ad libitum* for the whole duration of the experiment.

The rats were divided into 4 groups. Each group contained six males. The first group (Control) of rats (n = 6) served as the control one without selenium administration. The second group (C-GLU) of rats (n = 6) was administered by pure glucose (0.3 mg of glucose per kg of body weight / day). In the third group (SeN) of animals (n = 6), SeN (0.06 mg of Se per kg of body weight / day) was dosed. In the fourth group (SeN-GLU) of rats (n = 6), selenium nanoparticles bound with glucose (0.06 mg of Se and 0.3 mg of glucose per kg of body weight / day) was dosed. SeN and SeN-GLU were administered as a solution. SeN was injected into the animals at the same time of day using a pipette to accept completely all the content of solution. The differences in body weight between the different groups of rats were not significant (Fig.1).

All groups were fed with monodiet (kibbled wheat) containing up to 0.025 mg of selenium per kg of body weight / day. The rats were sacrificed after 10 days of the experiment (two hours from the last feeding). The samples of whole blood, erythrocytes, plasma, and liver were obtained from the animals and immediately subjected to the appropriate sampling analyzes.

2.2. Chemicals and pH measurement

Working solutions like buffers and standard solutions were prepared daily by diluting the stock solutions. Standards and other chemicals were purchased from Sigma-Aldrich (St. Louis, MO, USA) meets the specification of American Chemical Society (ACS), unless noted otherwise. Deionised water underwent demineralization by reverse osmosis using the instruments Aqua Osmotic 02 (AquaOsmotic, Tisnov, Czech Republic) and then it was subsequently purified using Millipore RG (Millipore Corp., USA, 18 MΩ) – MiliQ water.

2.3. Production of SeN and SeN-GLU

SeN and SeN-GLU were prepared according to the methodology of Chudobova *et al*. [43]. For the preparation of larger quantities of selenium nanoparticles, a 10-fold concentrated solution in a volume of 50 mL was prepared, in which up to 263 mg of sodium selenite and 240 μL of 3-mercaptopropionic acid (MPA) was used. The pH was adjusted to 9.0 due to higher stability of SeN.

During preparation of SeN-GLU, the entire process was repeated with the addition of 500 mg of glucose.

2.4. Size characterization of selenium nanoparticles

The average particle size and size distribution were determined by dynamic light scattering (DLS) with a Malvern Zetasizer (NANO-ZS, Malvern Instruments Ltd., Worcestershire, U.K.). Nanoparticles were dissolved in 1.5 mL of distilled water to concentration (1 mg.mL^{-1}). This solution was placed into a polystyrene latex cell and measured under following conditions: detector angle of 173°, wavelength of 633 nm, refractive index of 0.30, real refractive index of 1.33, and temperature of 25 °C. SeN size ranged from 33 to 79 nm and the size of SeN-GLU was in the range from 106 to 531 nm (Fig. 2 A and B). The nanodimensions of the synthesized selenium nanoparticles were confirmed by transmission electron microscopy (TEM) using the JEM-2010 (Jeol), Fig 2 A - a (SeN) and B - b (SeN-GLU)

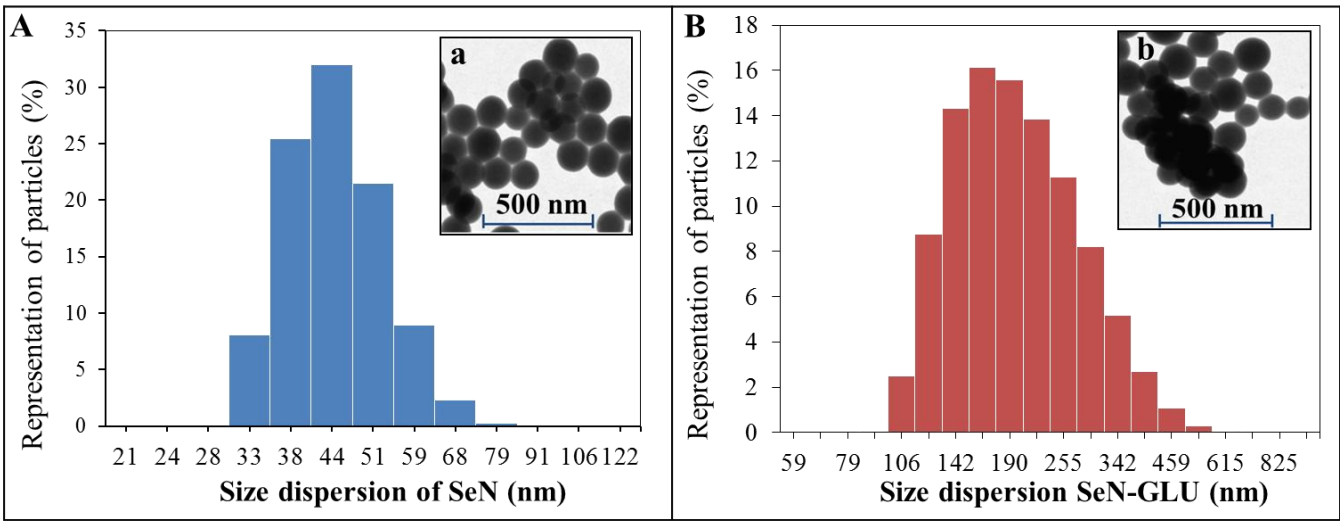

Figure 2. Percentage representation of various fractions of (**A**) SeN and (**B**) SeN-GLU measured by DLS and size confirmed by TEM in inserts (SeN(**a**) and SeN-GLU(**b**))

2.5. Preparation of plasma, erythrocyte and liver samples for determination of glutathione

The sample (300 µL) of blood plasma was taken and mixed with 300 µL of 10% TFA. Subsequently, the sample was centrifuged (24 000 g, 20 min, 4 °C). The supernatant was used for further analyses. The samples were stored on ice all the time.

The erytrocyte sample (100 mg of erytrocytes, fresh weight) was deeply frozen in liquid nitrogen. Next, 1.0 mL of 0.2 M phosphate buffer (pH 7.0) was added. The sample was vortexed for 15 min and centrifuged (25 000 g, 20 min, 4 °C). A volume of 300 µL of supernatant was taken and mixed with 300 µL of 10% TFA. Subsequently, the sample was centrifuged (24 000 g, 20 min, 4 °C). The supernatant was used for further analyses. The samples were stored on ice all the time.

The liver sample (1.0 g of liver, fresh weight) was deeply frozen in liquid nitrogen. Next, 1.0 mL of 0.2 M phosphate buffer (pH 7.0) was added. The sample was homogenized and vortexed for 15 min and centrifuged (25 000 g, 20 min, 4 °C). A volume of 300 μL of supernatant was taken and mixed with 300 μL of 10% TFA. Subsequently, the sample was centrifuged (24 000 g, 20 min, 4 °C). The supernatant was used for the analyses. The samples were stored on ice all the time.

2.6. HPLC-ED analysis of glutathione and its optimization using FIA-ED

For optimization of determination of reduced (GSH) and oxidized (GSSG) form of glutathione, a flow injection analysis with electrochemical detection (FIA-ED) system was used. It consisted of two chromatographic pumps Model 582 ESA (ESA Inc., Chelmsford, USA) with working range 0.001 - 9.999 $mL.min^{-1}$ and CoulArray electrochemical detector (Model 5600A, ESA, USA). Detector consisted of flow analytical chamber (Model 6210, ESA, USA). The chamber contains four analytical cells. One analytical cell contains two referent (hydrogen-palladium), and two counter electrodes and one porous graphite working electrode. Electrochemical detector is situated in control module, which is thermostated. Sample (20 μL) was injected by manual valve (Rheodyne, Oak Harbor, WA, USA). Flow rate of mobile phase was 1 mL min^{-1}.

GSH and GSSG was determined using HPLC-ED. The chromatographic system consisted of two solvent delivery pumps operating in the range of 0.001–9.999 mL min^{-1} (Model 582 ESA Inc., Chelmsford, MA, USA), and a chromatographic column Zorbax eclipse AAA C18 (150 × 4.6; 3.5 μm particle size; Agilent Technologies, Santa Clara, CA, USA) and a CoulArray electrochemical detector (Model 5600A, ESA, Chelmsford, MA, USA). The electrochemical detector includes three flow cells (Model 6210, ESA). Each cell consists of four working carbon porous electrodes, each one with auxiliary and dry Pd/H2 reference electrodes. Both of detector and reaction coil/column were thermostated. The sample (20 μL) was injected using autosampler (Model 542 HPLC, ESA). The samples were kept in the carousel at 8 °C during the analysis. The column was thermostated at 32 °C. Mobile phase consisted of 80 mM TFA (A) and methanol (B). The compounds of interest were separated by the following linear gradient: 0 → 1 min (3% B), 1 → 2 min (10% B), 2 → 5 min (30% B), 5 → 6 min (98% B). Mobile phase flow rate was of 1 $mL.min^{-1}$, working electrode potential of 900 mV. The time of analysis was for 20 min. Other experimental information is in papers [44-47].

2.7. Determination of antioxidant activity by FRAP method

The Ferric Reducing Antioxidant Power (FRAP) method is based on the reduction of complexes of 2,4,6-tripyridyl-*s*-triazine (TPTZ) with ferric chloride hexahydrate ($FeCl_3 \cdot 6H_2O$), which are almost colourless, and eventually slightly brownish. This chemical forms blue ferrous complexes after its reduction. Reagent preparation: Solution 1: 10 mM solution of TPTZ in 40 mM of hydrochloric acid. The solution 2: 20 mM, solution of ferric chloride hexahydrate in ACS purity water. Solution 3: 20 mM acetate buffer, pH 3.6. These three solutions (TPTZ, $FeCl_3$, acetate buffer) were mixed in a ratio 1:1:10. A 150 μL volume of reagent was injected into a plastic cuvette with the

subsequent addition of a 3 μL of sample. The absorbance was measured at 605 nm for 12 min. The difference between the absorbance for the last (12^{th}) minute and the second minute of the assay procedure was used for calculating of the antioxidant activity.

2.8. Determination of antioxidant activity by Free Radicals (FR) method

This method is based on the ability of chlorophyllin (the sodium-copper salt of chlorophyll) to accept and donate electrons with a stable change of maximum absorption. This effect is conditioned by an alkaline environment and the addition of catalyst. A 150 μL volume of reagent was injected into a plastic cuvette with the subsequent addition of a 6 μL sample. The absorbance was measured at 450 nm in the second minute of assay and for the last (12^{th}) minute. The difference between these two values was considered as an output value [48].

2.9. Determination of glucose

Glucose is oxidized by glucose oxidase to gluconolactone in the presence of oxygen. The resulting hydrogen peroxide is oxidized by 4-aminoantipyrine and phenol to quinone red in the presence of peroxidase. The intensity of generated red color is directly proportional to the concentration of glucose and can be photometrically determined. 200 μL of reagent (Greiner, Germany, 0.1 M phosphate buffer of pH 7.5, 0.75 mM phenol, 0.25 mM 4-aminoantipyrin, glucose oxidase ≥ 15kU / L peroxidase ≥ 1.5 U / L) was placed into plastic cuvette followed by 20 μL of the sample. The absorbance was measured at $\lambda = 505$ nm after an incubation lasting for 10 min. The absorbance values of reagents and absorbance values after 10-min incubation with the sample were used to calculate the glucose content.

2.10. Preparation of plasma, erythrocytes and liver samples for determination of MT

A 100 mg of sample (plasma or erythrocytes) was weighed into the eppendorf tube and immediately deeply frozen in a liquid nitrogen for 2 min, and 1 mL of phosphate buffer (200 mM, pH 7) was added. The sample was homogenized using ultrasound needle for 2 min then vortexed for 15 min and centrifuged (25 000 g, 20 min at 4 °C). After the centrifugation, the supernatant (10 μL) was taken and mixed with 990 μL of phosphate buffer (200 mM, pH 7) and denaturated at 99 °C for 20 min then placed into the thermomixer at 300 rpm (Eppendorf thermomixer comfort, Germany). After the denaturation, the erythrocyte samples were centrifuged (25 000 g, 20 min at 4° C) and the concentration of total protein was spectrophotometrically determined (Mindray, BS 200, Shenzen, Peoples Republic China). The concentration of MT was determined by DPV. The samples were stored on the ice all the time.

A sample (1.0 g of liver, fresh weight) was deeply frozen by liquid nitrogen. After that, a 1 mL of 0.2 M phosphate buffer (200 mM, pH 7.0) was added. The sample was homogenized and vortexed for 15 min and centrifuged (25 000 g, 20 min at 4 °C). After the centrifugation, the supernatant (10 μL)

was taken and mixed with 990 μL of phosphate buffer (200 mM, pH 7.0) and denaturated at 99 °C for 20 min, at 300 rpm in the thermomixer (Eppendorf thermomixer comfort, Germany). After the denaturation, liver samples were centrifuged (25 000 g, 20 min at 4 °C) and measured the concentration of total protein using the equipment (Mindray, BS 200, Shenzen, Peoples Republic China). The concentration of MT was measured by DPV. The samples were stored on the ice all the time.

2.11. Determination of MT

DPV measurements were performed with a 747 VA Stand instrument connected to 693 VA Processor and an 695 Autosampler (Metrohm, Switzerland) using a standard cell with three electrodes and cooled sample holder and the measurement of cell to 4 °C (Julabo F25, JulaboDE). A hanging mercury drop electrode (HMDE) with a drop area of 0.4 mm^2 was the working electrode. An Ag/AgCl/3M KCl electrode was the reference and glassy carbon electrode was the auxiliary. For data processing VA Database 2.2 by Metrohm, CH was used. The analyzed samples were deoxygenated prior to the measurements by purging with argon (99.999 %) and saturated with water for 120 s. Brdicka supporting electrolyte containing 1 mM of $Co(NH_3)_6Cl_3$ and 1 M ammonia buffer (NH_3(aq) and NH_4Cl, pH = 9.6) was used. The supporting electrolyte was exchanged after each analysis. The parameters of the measurement were as follows: initial potential of -0.7 V, end potential of -1.75 V, modulation time for 0.057 s, time interval for 0.2 s, step potential of 2 mV, modulation amplitude -250 mV, E_{ads} = 0.0 V, volume of injected sample: 10 μL, volume of measurement cell 2.0 mL (10 μL of sample, 1990 μL of Brdicka solution) [49-52].

2.12. Microwave digestion for atomic absorption spectrometry (AAS)

A 10 μL of plasma or blood were pipetted into digestion vials and 10 mg of homogenized liver or intestine and feed were weighed into digestion vials. Nitric acid (65 %) and hydrogen peroxide (30 %) were used as the digestion mixture. A 500 μL of volume of digestion mixture was used, while the ratio between nitric acid and hydrogen peroxide was always 7:3 (350 μL HNO_3 and 150 μL H_2O_2). The samples were digested by Microwave 3000 (Anton Paar GmbH, Austria), rotor MG-65. The program begins and ends with the same ten-minute-long-step and beginning with the power of 50 W and ending with the power of 0 W (cooling). Microwave power was of 100 W in the main part of the programs (for 30 min), 140 °C.

2.13. Determination of selenium by AAS

Selenium was determined by 280Z Agilent Technologies atomic absorption spectrometer (Agilent, Germany) with electrothermal atomization. Selenium ultrasensitive hollow cathode lamp (Agilent, Germany) was used as the radiation source (lamp current 10 mA). The spectrometer was operated at 196.0 nm resonance line with spectral bandwidth of 1.0 nm. The sample volume of 20 μL

was injected into the graphite tube. The flow of inert gas (argon) was of 300 $mL \cdot min^{-1}$. Zeeman background correction was used with field strength of 0.8 T. Selenium was determined in the presence of palladium chemical modifier.

2.14. Sample preparation for electrochemical determination of free zinc and copper

0.1 g of the tissue or 100 µL of plasma was transferred into a test tube and then deep-frozed by liquid nitrogen to disrupt cells. The frozen tissues were mixed with extraction buffer (100 mM potassium phosphate, pH 7) to a final volume of 1.0 mL and homogenised using hand-operated homogenizer ULTRA-TURRAX T8 (IKA, Königswinter, Germany) placed in an ice bath for 3 min at 25 000 rpm. The homogenate was centrifuged at 10 000 g for 15 min and at 4 °C (Eppendorf 5402, Hamburg, Germany). The resulting supernatant was used for analysis of free zinc and copper.

2.15. Electrochemical determination of Zn and Cu

Determination of zinc by DPV was performed with 797 VA Computrace instrument connected to 813 Compact Autosampler (Metrohm, Switzerland), using a standard cell with three electrodes. The HMDE with a drop area of 0.4 mm^2 was the working electrode. An Ag/AgCl/3M KCl electrode was the reference and platinum electrode was auxiliary. For data processing 797 VA Computrace software by Metrohm CH was employed. The analyzed samples were deoxygenated prior to measurements by purging with argon (99.999%). Acetate buffer (0.2 M CH_3COONa and CH_3COOH, pH 5) as a supporting electrolyte was used. The supporting electrolyte was exchanged after each analysis. The parameters of the measurement were as follows: initial potential of -1.2 V, end potential -0.7 V, deoxygenating with argon 90 s, deposition 420 s, time interval 0.04 s, step potential 5 mV, modulation amplitude -25 mV, adsorption potential -1.2 V, volume of injected sample: 15 µl, volume of measurement cell 2.0 mL (15 µL of sample and 1985 µL of acetate buffer).

2.16. Statistic analyses

The data were statistically processed using STATISTICA.CZ, version 10.0 (Czech Republic). The results were expressed as a mean from 5 measurements ± standard deviation. Statistical significance was determined by the examining of basic differences among groups using ANOVA and Scheffé's method for the parameters GSH; GSSG; Se; Cu, Zn, glucose; FR; FRAP; MT. The differences with $P < 0.05$ were considered as significant. For HPLC-ED and FIA-ED analysis of GSH and GSSG mathematical analysis of the data and their graphical interpretation were realized by Microsoft Excel®, Microsoft Word® and Microsoft PowerPoint®. Results were expressed as mean ± standard deviation (S.D.) unless noted otherwise. The detection limits (3 signal/noise, S/N) were calculated according to Long and Winefordner [53] , whereas N was expressed as standard deviation of noise determined in the signal domain unless stated otherwise.

3. RESULTS

3.1. Spectrophotometric determination of antioxidant activity

In the experiment, the influence of two selenium forms - SeN and SeN-GLU - on the antioxidant status of the rats was observed. Blood plasma (Fig.3A, B, C), erythrocytes (Fig.3D, E, F) or whole blood as well as liver (Fig.3G, H, I) were analyzed.

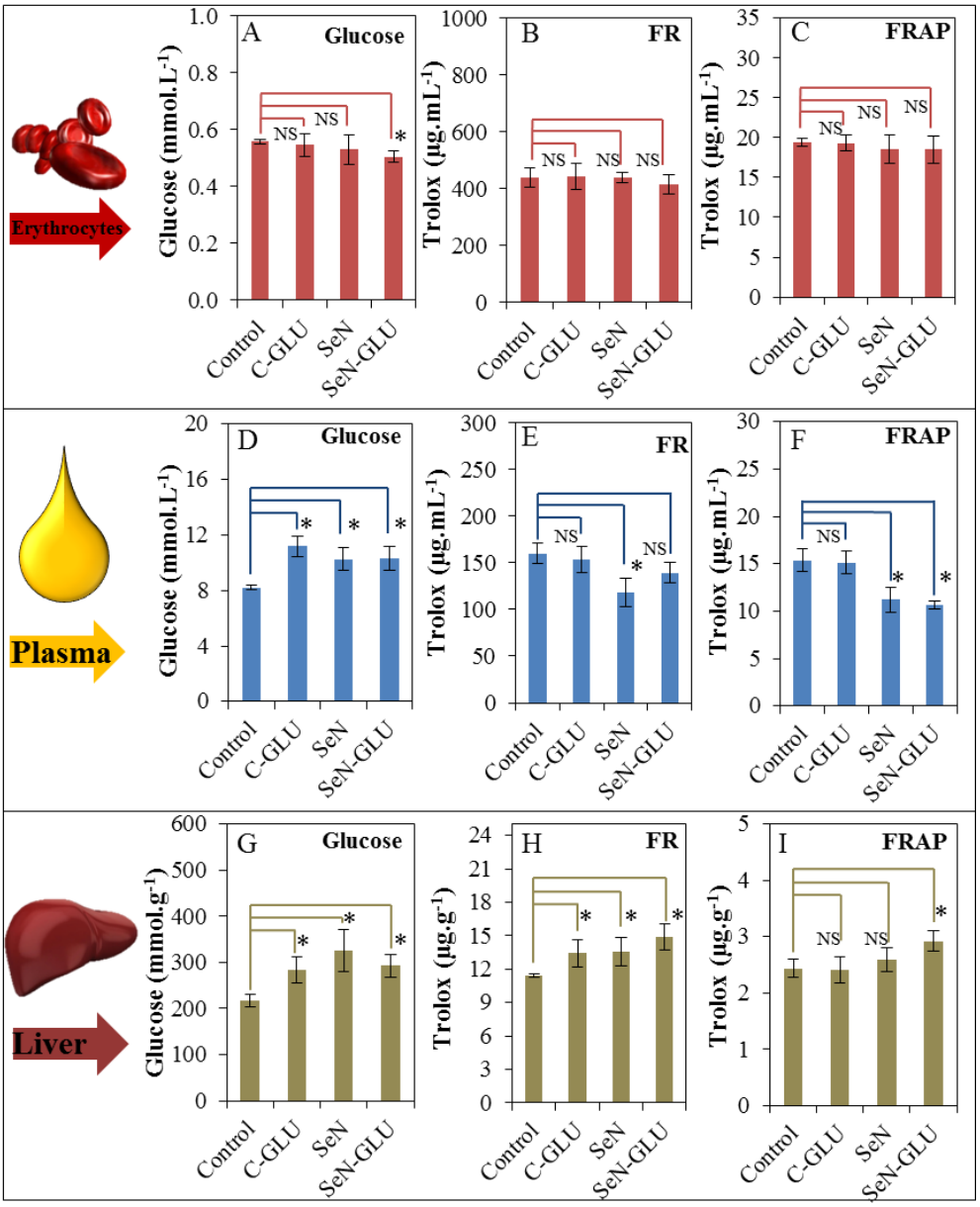

Figure 3. The influence of 10 days feeding with SeN (0.06 mg of Se per kg of body weight / day) and SeN-GLU (0.06 mg of Se and 0.1 mg of glucose per kg of body weight / day) on the level of glucose (**A**); and antioxidant activities measured by FR method [54] (**B**) and FRAP method (**C**) in erythrocytes, plasma and livers of rats. All data represent mean ± s.d. from 5 measurements, NS, not significant, * $P < 0.05$. Other experimental details see in Material and Methods section.

The glucose level was determined and 2 methods (FR and FRAP) were used to evaluate the antioxidant activity. In the case of erythrocytes, the glucose level was insignificantly decreased in the SeN group. In SeN-GLU group, the glucose level was decreased significantly (by 9%) (Fig.3A).

In samples of rat plasma, significant increase in glucose concentration was determined in all groups (by 36% in C-GLU; by 25% in SeN, and by 26% in SeN-GLU) compared to the control one (Control) – (Fig. 3D), resulting in elevated blood glucose in C-GLU, SeN and SeN-GLU.

The comparison of liver samples showed that the higher glucose value was measured in the second control group (C-GLU), which was increased by 31% ($P < 0.05$) compared to the control one. SeN and SeN-GLU groups had higher content of glucose by 50% ($P < 0.05$) and by 34% ($P < 0.05$), respectively (Fig.3G).

During the evaluation of the antioxidant activities measured by both the FR and FRAP methods, insignificant differences between the experimental and control groups of animals was observed in the erythrocytes. The differences ranged from 1 to 5 % between the experimental groups (Fig.3B, C). During the evaluation of the antioxidant potential in plasma, a significant decrease in antioxidant activity measured using FR by 27% ($P < 0.05$) was observed in SeN, and insignificant decrease by 13% in SeN-GLU (Fig.3E). Concerning FRAP method a significant decrease by 27% ($P < 0.05$) in SeN and by 30% in SeN-GLU was observed (Fig.3F).

When evaluating the antioxidant activity using FR method in liver samples, a significant increase by 18% ($P < 0.05$) in C-GLU, by 19% ($P < 0.05$) in SeN and by 30% ($P < 0.05$) in SeN-GLU group was observed (Fig. 3H). During the evaluation of antioxidant activity using FRAP method in liver samples, the insignificant increase by 7% in SeN and significant increase by 20% ($P < 0.05$) in SeN-GLU (Fig. 3I) was determined.

Generally, the antioxidant activity of SeN and SeN-GLU groups was decreased in plasma and increased in liver in comparison with controls.

3.2. Optimization of electrochemical detection for HPLC-ED analysis of GSH and GSSG

Further, we performed the optimization of electrochemical detection of reduced and oxidized glutathione for HPLC-ED analyzis. For electrochemical experiment, flow injection analysis setup with electrochemical detector (FIA-ED) containing four analytical cells was employed.

3.2.1 Optimization of concentration of TFA and AA in a mobile phase for GSH determination using FIA-ED

Firstly, the electrochemistry was utilized to monitor an effect of mobile phase on electrochemical response of GSH using FIA-ED. As it can be seen in Fig. 4 (A), two mobile phases (TFA – trifluoracetic acid, AA-Acetic Acid) were tested in 3% addition into acetonitrile (ACN, v/v). Analyzes were performed within the potential range of 100 – 1100 mV, and it was shown that TFA supports the analysis at the ideal potential (1100 mV) more than AA (peak height of GSH in TFA was

59.45 µA and 20.48 µA in AA). Therefore, 3% addition of ACN to TFA (v/v) was chosen as beneficial to increase sensitivity in subsequent analyses.

Although, 80 mM TFA with 3% addition of ACN showed a relatively good detector response for GSH (59.45 µA), we decided to test various concentrations of TFA and AA due to their ability to enhance the sensitivity of detection. Firstly, we tested various concentrations of TFA, because TFA has shown to have the greatest effect on peptide detection from our previous studies [55,56]. Hence, for further optimization experiments we utilized TFA within a concentration range of 10-160 mM (3% addition of ACN (v/v)) and potentials within range of 100 – 1100 mV (Fig.4 B).

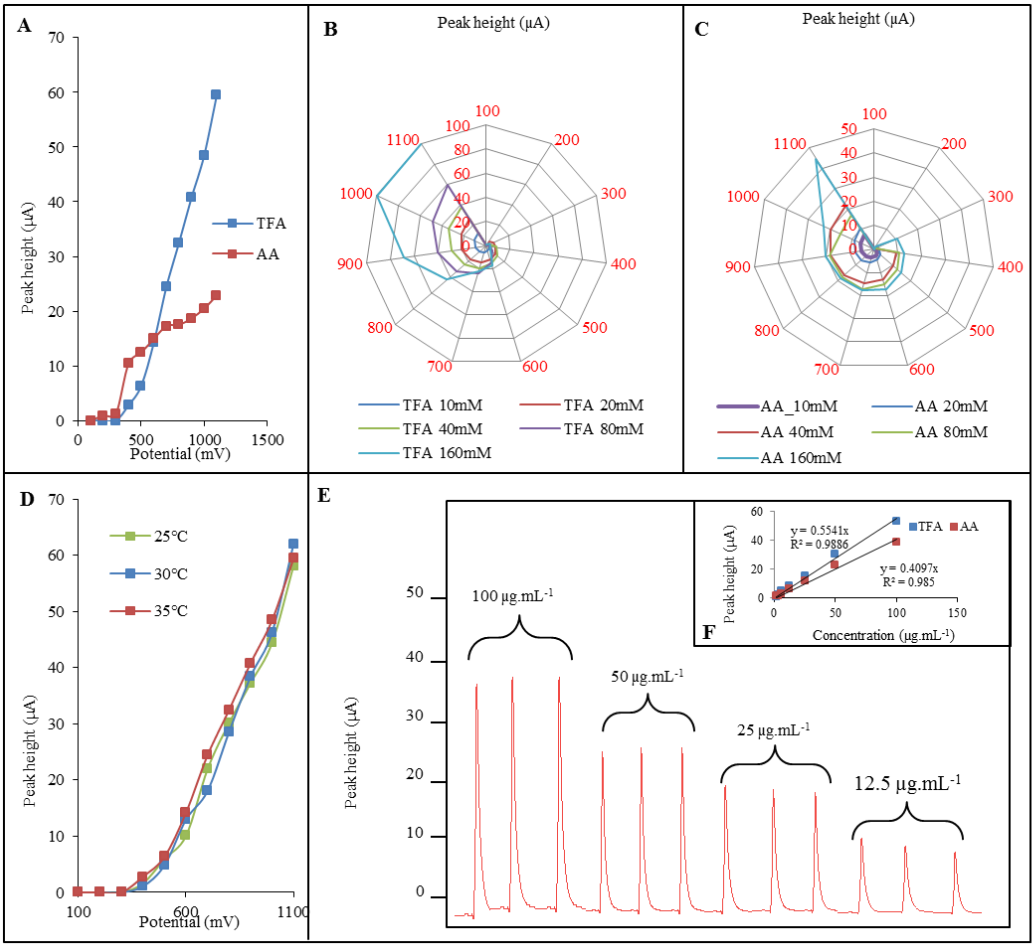

Figure 4. Optimization of FIA-ED of GSH. Applied concentration of GSH for analyzes was 100 µg.mL^{-1}. Expression of influence of addition of mobil phases on amperometric signal of the GSH. TFA–Trifluoracetic Acid , AA –Acetic Acid (A). Hydrodynamic voltammograms of GSH measured under optimized conditions (TFA or AA with 3% addition of ACN (v/v) in potential range 100 – 1100 mV). Optimization of potential for detection (100 – 1100 mV) of the GSH, and its behavior under influence of different concentrations (10, 20, 40, 80, and 160 mM) of both TFA (B) and AA (C). The influence of temperature (25-35 °C) on detection of GSH (D). Array record of GSH calibration curve measured in TFA within the range from 3.7 to 100 µg.mL^{-1}(E). Calibration curve measured within range from 3.5 to 100 µg.mL^{-1} using best conditions such as potential of 1100 mV and 160 mM TFA or 160 mM AA with 3% addition of ACN (F).

As it is obvious from Fig. 4B, already the lowest concentration of TFA (10 mM) has influenced the detection of GSH in terms of the sensitivity. Optimal potential was determined at 1100 mV showing GSH peak with a height of 12.35 μA. After application of 20 mM TFA, the optimal potential was also 1100 mV (peak height 26.53 μA). Similar situation was in the case of 40 mM TFA (peak height 38.03 μA) and 80 mM TFA (peak height 59.42 μA). The increase of the TFA concentration to 160 mM led to the significant change in electrochemical behaviour of GSH. Optimal potential was determined already at 1000 mV (peak height 99.98 μA).

In the case of using the acetic acid as the mobile phase, the similar behavior was observed, but the peak heights were generally lower. Concentrations of AA in the range 10-160 mM (3% addition of ACN (v/v)) and potentials within range 100–1100 mV were used (Fig.4 C). As it is obvious from Fig. 4C, the lowest concentration of AA (10 mM) when using optimal potential at 1100 mV showed GSH peak with height of 6.90 μA. In case of all AA concentrations optimal potential was 1100 mV and the peak peak heights were as follows: 10.01 μA (20 mM) 21.73 μA (40 mM), 22.57 μA (80 mM), and 45.01 μA (160 mM).

Sensitivity of the electrochemical detector may be more influenced by factors including the type of electrolyte in the mobile phase, concentration, pH and, in particular, applied potential. TFA was used as an ion-pair reagent, which provides the best separation conditions in the parameters mentioned above, and at the concentration of 80 mM it is also extremely suitable electrolyte for the detection of thiols. For further optimization experiments we utilized TFA 80 mM (3% addition of ACN (v/v)) and potentials within range 100 – 1100 mV in using different temperature within range between 25-35 °C (Fig. 4D). An ideal temperature for detection of GSH was determined at 35 °C (Fig. 4D).

In ideal manner, the working electrode should be immersed to the supporting electrolyte and should give response only to the analyzed substance in a thermodynamically defined, potential-dependent fashion [57]. In our case, hydrodynamic voltammetry was carried out within the potential range from 100 to 1100 mV (Fig. 4B,C). It clearly follows from the results obtained that the current response increases relatively slowly up to reaching interval of redox potential (800 mV). After reaching this "inflection point", the current response increases rapidly to high oxidation potential, where maximal detection potential (1100 mV) was achieved as the ideal for GSH analyses in the TFA (peak height 99.98 μA) and in the AA (peak height 45.01 μA).

After we optimization of the electrochemical analysis of the GSH, calibration curve was measured within the concentration range from 1.5 to 100 $\mu g.mL^{-1}$ and is shown in Fig. 4E, F. The linear dependence of GSH signal on its applied concentration ($y=0.5541$, $R^2=0.989$) in the TFA and ($y=0.4097$, $R^2=0.985$) in the AA mobile phases were obtained in the above-mentioned concentration range. Using the optimal conditions, we were able to determine the detection limit (3 S/N) of the GSH measured in TFA as 0.2 $\mu g.mL^{-1}$. Other analytical parameters are shown in Tab. 1. Limit of quantification (10 S/N) was determined as 0.5 $\mu g.mL^{-1}$.

Using the optimal conditions, we were also able to determine the LOD (3 S/N) of the GSH measured in AA as 0.2 $\mu g.mL^{-1}$. LOQ (10 S/N) was determiend as 0.7 $\mu g.mL^{-1}$.Other analytical parameters are shown in Tab. 2.

Table 1. Parameters of electrochemical analysis of GSH in TFA, where Mr stands for molecular mass, R^2 for coefficient of determination, LOD for limit of detection (3 S/N), LOQ for limit of quantification (10 S/N) and RSD for relative standard deviation calculated from 3 measurements of GSH standard (100 μg.mL^{-1} ; injection of 20 μL of sample).

Compound	Mr	Regression equation	Linear dynamic range	R^2	LOD	LOQ	RSD
	g.mol^{-1}		(μg.mL^{-1})		(μg.mL^{-1})	(μg.mL^{-1})	%
GSH	307.3	y = 0.5541x	0.5 – 100.0	0.989	0.2	0.5	2.2

Table 2. Parameters of electrochemical analysis of GSH in AA, where Mr stands for molecular mass, R^2 for coefficient of determination, LOD for limit of detection (3 S/N), LOQ for limit of quantification (10 S/N) and RSD for relative standard deviation calculated from 3 measurements of GSH standard (100 μg.mL^{-1} ; injection of 20 μL of sample).

Compound	Mr	Regression equation	Linear dynamic range	R^2	LOD	LOQ	RSD
	g.mol^{-1}		(μg.mL^{-1})		(μg.mL^{-1})	(μg.mL^{-1})	%
GSH	307.3	y = 0.4097x	0.7 – 100.0	0.985	0.2	0.7	0.4

3.2.2 Optimization of concentration of TFA and AA in a mobile phase for GSSG determination using FIA-ED

Similarly, as it was performed in the GSH determination also in the GSSG determination, two mobile phases (TFA and AA) were tested in 3% addition into ACN (Fig.5A). Analyzes were performed again within the potential range of 100 – 1100 mV, and it was shown that TFA supports the analyzis at the ideal potential (1100 mV) much more than AA (peak height of GSH was in TFA 43.05 μA and in AA 12.23 μA). Therefore, 3% addition of ACN into TFA (v/v) was also chosen as beneficial to increase sensitivity in subsequent analyses.

As it is of sensitivity. Optimal potential was determined at 1100 mV showing GSSG peak with a height of 10.63 μA. After application of 20 mM TFA, the optimal potential was also 1100 mV (peak height 18.18 μA). Similar situation was in the case of 40 mM TFA (peak height 29.88 μA) and 80 mM TFA (peak height 42.78 μA). The increase of the TFA concentration to 160 mM led to the further increase in electrochemical signal of GSSG. Optimal potential was determined again at 1100 mV (peak height 69.30 μA).

In the case of using of acetic acid as the mobile phase, the similar behavior was observed, but the peak heights were generally lower. Concentrations of AA in the range 10-160 mM (3% addition of ACN (v/v)) and potentials within range 100 – 1100 mV were used) (Fig.5C). As it is obvious from Fig. 5C, the lowest concentration of AA (10 mM) when using optimal potential at 1100 mV showed GSSG peak with height of 3.97 μA. In case of all AA concentrations optimal potential was 1100 mV and the

peak heights were as follows: 7.98 µA (20 mM) 10.23 µA (40 mM), 10.91 µA (80 mM), and 20.71 µA (160 mM).

For further optimization experiments as in the case of GSH we utilized TFA 80 mM (3% addition of ACN (v/v)) and potentials within range 100 – 1100 mV in using different temperature within range between 25-35 °C (Fig. 5D). Ideal temperature for detection of GSH was determined at 35 °C (Fig. 5D).

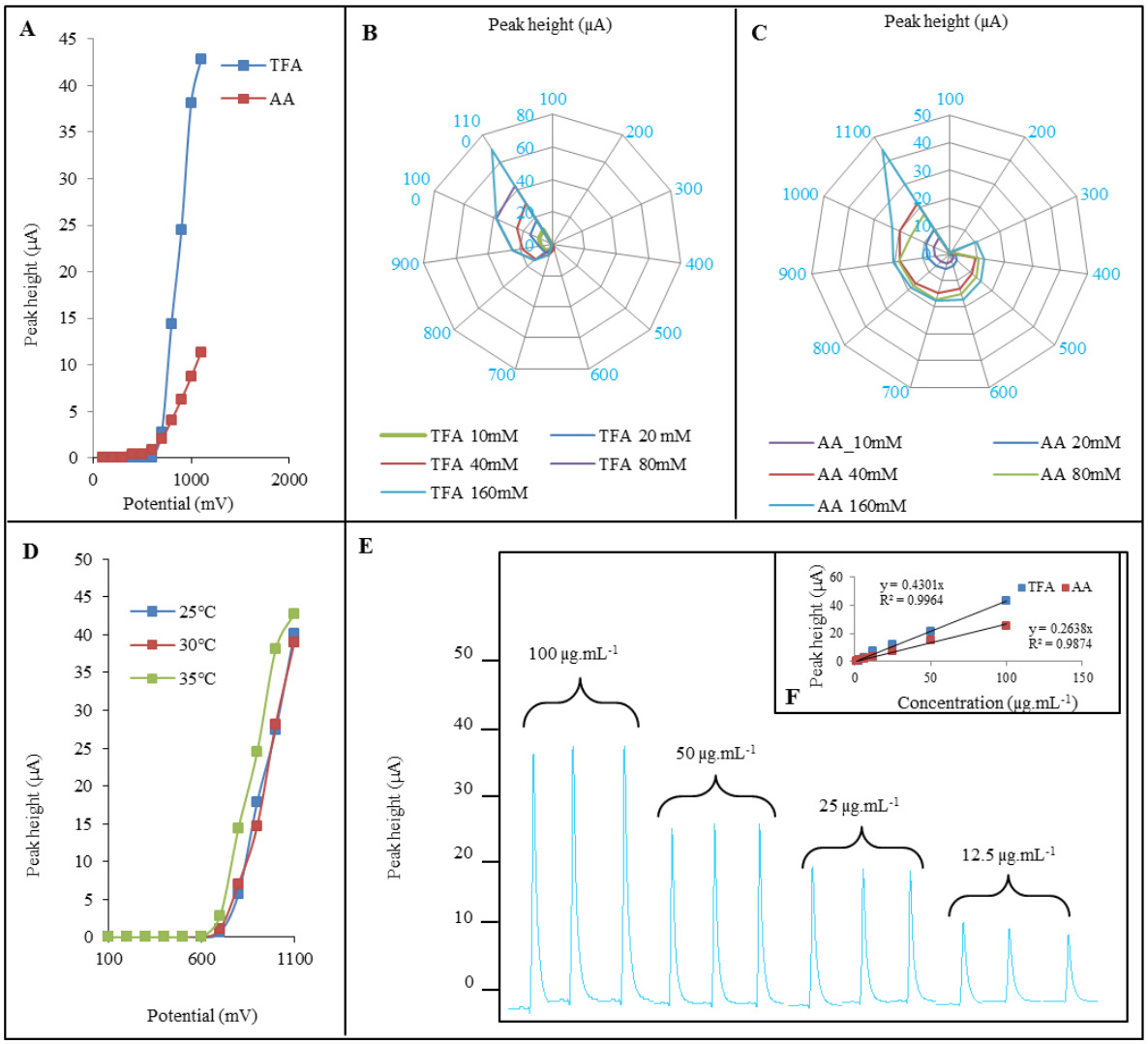

Figure 5. Optimization of FIA-ED of GSSG. Applied concentration of GSSG for analyzes was 100 µg.mL^{-1}. Expression of influence of addition of mobil phases on amperometric signal of the GSH. TFA–Trifluoracetic Acid, AA –Acetic Acid (A). Hydrodynamic voltammogram of GSSG measured under optimized conditions (TFA or AA with 3% addition of ACN (v/v) in potential range 100 – 1100 mV). Optimization of potential for detection (100 – 1100 mV) of the GSSG and its behavior under influence of different concentrations (10, 20, 40, 80, and 160 mM) of both TFA (B) and AA (C). Optimization the temperature influence (25-35 °C) on detection of GSSG (D). Array record of GSSG calibration curve in TFA measured within the range from 3.7 to 100 µg.mL^{-1} (E). Calibration curve was measured within range from 3.5 to 100 µg.mL^{-1} using best conditions such as potential of 1100 mV and 160 mM TFA or 160 mM AA with 3% addition of ACN (F).

After we optimized the electrochemical analysis of the GSSG, calibration curve was measured in the TFA within the range from 1.5 to 100 $\mu g.mL^{-1}$. From these data we constructed the calibration curve, which is shown in (Fig. 5 E, F). The linear dependence of GSSG signal on its applied concentration (y =0.4301, R^2 =0.996) was obtained in the above-mentioned concentration range. Using the optimal conditions, we were able to determine the detection limit (3 S/N) of the GSSG as 0.2 $\mu g.mL^{-1}$. Limit of quantification (10 S/N) was estimated as 0.6 $\mu g.mL^{-1}$. Other analytical parameters are shown in Tab.3.

Table 3. Parameters of electrochemical analysis of GSSG in (TFA), where Mr stands for molecular mass, R^2 for coefficient of determination, LOD for limit of detection (3 S/N), LOQ for limit of quantification (10 S/N) and RSD for relative standard deviation calculated from 3 measurements of GSH standard (100 $\mu g.mL^{-1}$; injection of 20 µL of sample).

Compound	Mr	Regression equation	Linear dynamic range	R^2	LOD	LOQ	RSD
	$g.mol^{-1}$		($\mu g.mL^{-1}$)		($\mu g.mL^{-1}$)	($\mu g.mL^{-1}$)	%
GSSG	612.6	y = 0.4301x	0.6 – 100.0	0.996	0.2	0.6	0.4

After we optimized the electrochemical analysis of the GSSG, calibration curve was measured in the AA within the range from 1.5 to 100 $\mu g.mL^{-1}$. From these data we constructed the calibration curve, which is shown in (Fig. 5E, F). The linear dependence of GSSG signal on its applied concentration (y=0.2638, R^2=0.9874) was obtained in the above-mentioned concentration range. Using the optimal conditions, we were able to determine the detection limit (3 S/N) of the GSSG as 0.3 $\mu g.mL^{-1}$. Limit of quantification (10 S/N) was determined as 1 $\mu g.mL^{-1}$. Other analytical parameters are shown in Tab.4.

Table 4. Parameters of electrochemical analysis of GSSG in the Acetic Acid (AA), where Mr stands for molecular mass, R^2 for coefficient of determination, LOD for limit of detection (3 S/N), LOQ for limit of quantification (10 S/N) and RSD for relative standard deviation calculated from 3 measurements of GSH standard (100 $\mu g.mL^{-1}$; injection of 20 µL of sample).

Compound	Mr	Regression equation	Linear dynamic range	R^2	LOD^3	LOQ^4	RSD
	$g.mol^{-1}$		($\mu g.mL^{-1}$)		($\mu g.mL^{-1}$)	($\mu g.mL^{-1}$)	%
GSSG	612.6	y = 0.2638x	1.0 – 100.0	0.987	0.3	1.0	0.2

3.2.3 Optimization of HPLC-ED analysis of GSH and GSSG using array records

Typical chromatogram of GSH and GSSG measured by HPLC coupled with eight-channel electrochemical detector is shown in Fig.6. The GSH and GSSG were separated by isocratic elution

where the ratio of TFA and ACN was 99:1 (v/v). Based on the optimisation steps by FIA-ED, the mobile phase, which consisted of (A) 80 mM TFA and (B) 160 mM TFA, was used for separation and detection of GSH and GSSG. The compounds of interest were separated by the following linear gradient: 0 → 7 min (3% B), 7 → 15 min (15% B), 15 → 25 min (30% B), 25 → 33 min (98% B). Flow rate of the mobile phase was 1 $mL.min^{-1}$ and working electrode potential was set to 400- 1100 mV. We studied the effect of the applied potential on the working electrode set separately for GSH and GSSG, which were designed for chromatograms of GSH and GSSG.Tested potentials were 400, 500, 600, 700, 800, 900 and 11000 mV. The responses detected at 400 mV were insignificant; however, when the potential reached 500 mV, detectable signals for GSH and GSSG were observed. While the GSH signal markedly increased from 600 mV, the GSSG signal significantly increased from 700 to 1100 mV. This is probably due to the requirement for greater power for partial dissociation of the -S-S- group on the surface of the working electrode, in comparison to the relatively easily accessible -SH moiety of GSH. This work shows that HPLC-ED method that we developed is very suitable for the purpose of analyzing the content of thiols in varios types of matrices.

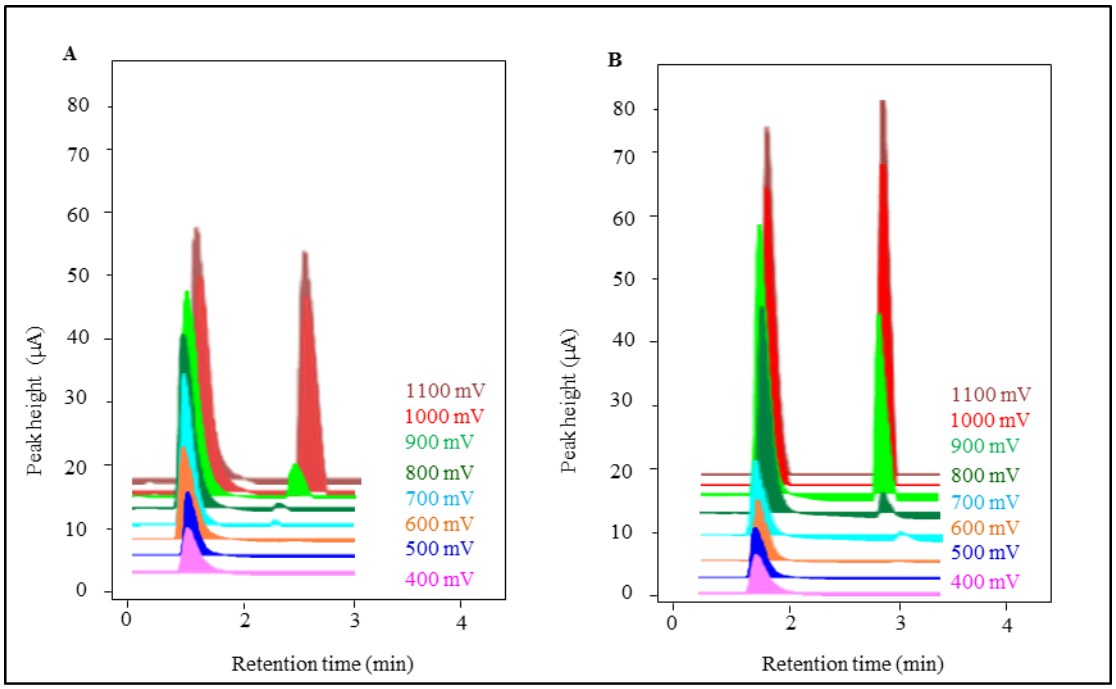

Figure 6. Array records of GSH and GSSG (100 $\mu g.mL^{-1}$) measured under optimized conditions (80 mM and 160 mM TFA with 3% addition of ACN (v/v) in potential range of 400–1100 mV) (**A**) 80 mM TFA (**B**) 160 mM TFA

3.3 HPLC-ED analysis of GSH and GSSG

Another monitored antioxidant parameter, which has a direct correlation with selenium and indicates the antioxidant potential of the organism, is the level of GSH and GSSG. GSH and GSSG values in a whole blood are shown in Fig.7A. In the analysis of whole blood, a significant increase of GSH by 41 % ($P < 0.05$) was observed in the SeN-GLU group compared with the control one. Higher

levels of GSH were also observed in the C-GLU and SeN groups by 17 % and by 12 %, respectively, but without statistical significance. In the case of GSSG, the highest concentration of SeN-GLU (an increase of 23%; P <0.05 compared with the control group) was observed. For the SeN group, a decrease in GSSG by 13% (P <0.05) without any significant evidence was observed, on the other hand, a significant increase by 22% (P <0.05) was observed for the SeN-GLU group.

In the assessing of GSH in erythrocytes, a linear increase was observed for each group. An increase by 8% in the C-GLU group, by 14% in the SeN group and a significant increase by 19% (P <0.05) in the SeN-GLU group of rats was recorded. The nonsignificant changes in GSSG content was the lowest in the C-GLU group (a reduction by 16%) compared with control one). The amount of GSSG was the highest in the SeN group (an increase by 21%). The concentrations of GSH and GSSG in erythrocytes are shown in Fig. 7B.

In the liver, a decrease in both forms of glutathione was observed. The highest value was detected in the control group of rats. Conversely, the lowest concentrations of GSH were recorded in two experimental groups of SeN a SeN-GLU (a reduction by 27%, and by 15%, respectively, (P < 0.05)). In case of GSSG, the highest level was observed in the control group similarly to GSH. Significantly, the lowest value of GSSG compared with a control group of rats proved SeN (by 27%; P < 0.05) and SeN-GLU (by 26%; P < 0.05). The measured concentrations of GSH and GSSG in the liver are shown in Fig. 7C

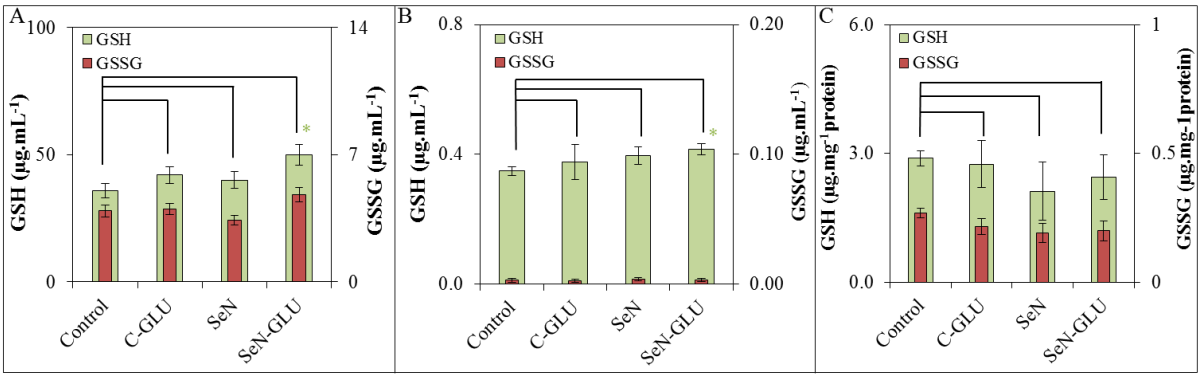

Figure 7. Influence of SeN and SeN-GLU on the level of reduced (GSH) and oxidized form (GSSG) of glutathions in a whole blood (**A**); erythrocytes (**B**) and liver (**C**). All data represent mean ± s.d. from 5 measurements, NS, not significant, * P < 0.05. Other experimental details see in Material and Methods section.

3.4. Analysis of Se using AAS

In all groups of rats, the selenium content of whole blood, plasma, and liver was monitored (Fig.8). In the case of the whole blood, a significant increase was detected in the concentration of selenium in both groups SeN by 114% (P < 0.05) and in SeN-GLU by 52% (P < 0.05) compared with the control group of rats (Fig.8A).

In the blood plasma, nonsignificant changes were detected. The highest selenium concentration was measured in the SeN-GLU group (Fig.8B). In the assessing of the selenium

concentration in the liver, the highest selenium content was found out in the group of SeN-GLU. In the comparison with the C-GLU control group, the selenium content was significantly increased by 29% ($P < 0.05$) (Fig.8C).

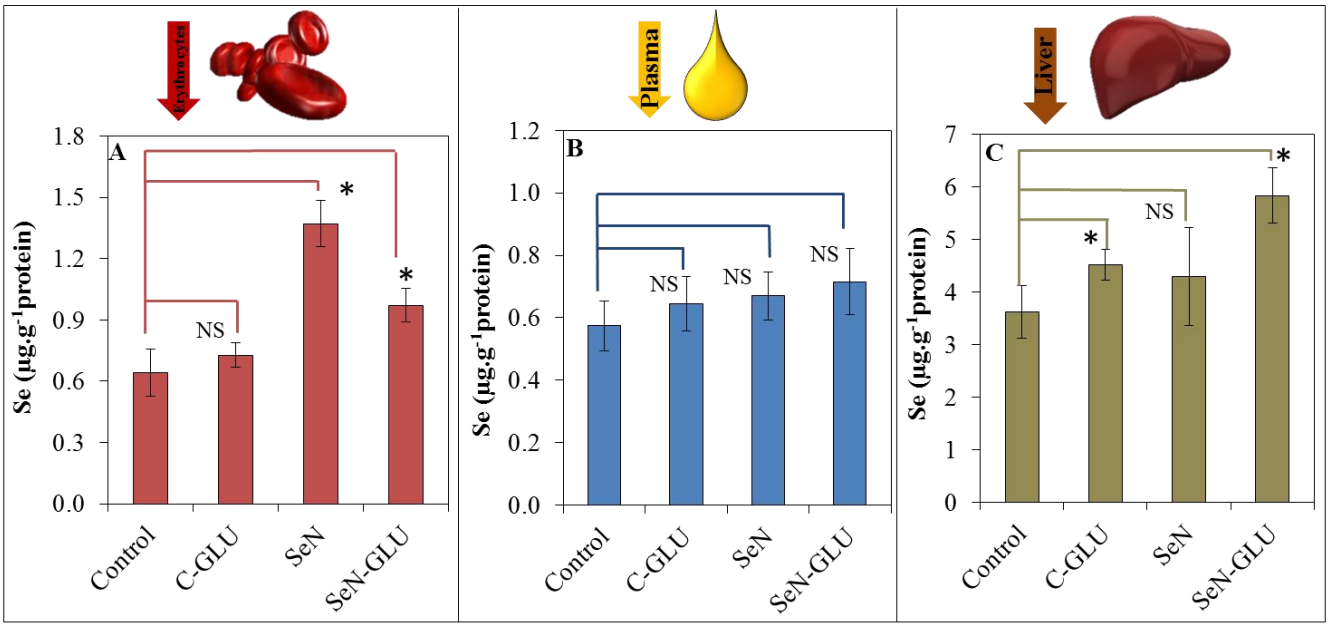

Figure 8. Influence of SeN and SeN-GLU on selenium concentration in a whole blood (**A**), plasma (**B**) and liver (**C**). All data represent mean ± s.d. from 5 measurements, NS, not significant, * $P < 0.05$. Other experimental details see in Material and Methods section.

3.5. Analysis of MT using DPV

Next, the level of MT, [58] which has the ability to bind heavy metals within the cells, in the blood plasma, erythrocytes and liver of rats was assessed. DPV was used for measurement. Typical voltammograms of blood, erythrocyte and liver samples of 4 different groups of rats are shown in Fig.9A, B, C. Calibration curve of MT in phosphate buffer is shown in Fig.9D. CAT2 signal was used for preparation of calibration curve.

In erythrocytes, MT concentration increased in C-GLU group by 80% ($P < 0.05$); in SeN by 120% ($P < 0.05$) and in SeN-GLU by 238% ($P < 0.05$). MT values in plasma linearly increased. In C-GLU group MT values increased insignificantly by 19%, in SeN group by 31% ($P < 0.05$) and the highest value was observed in the SeN-GLU group (an increase by 59%; ($P < 0.05$). The same trend of MT values as in plasma was observed in the liver, where a significant increases were observed in C-GLU group by 58% ($P < 0.05$), in SeN group by 91%, and the highest increase by 186% ($P < 0.05$) was observed in the SeN-GLU group (Fig. 9).

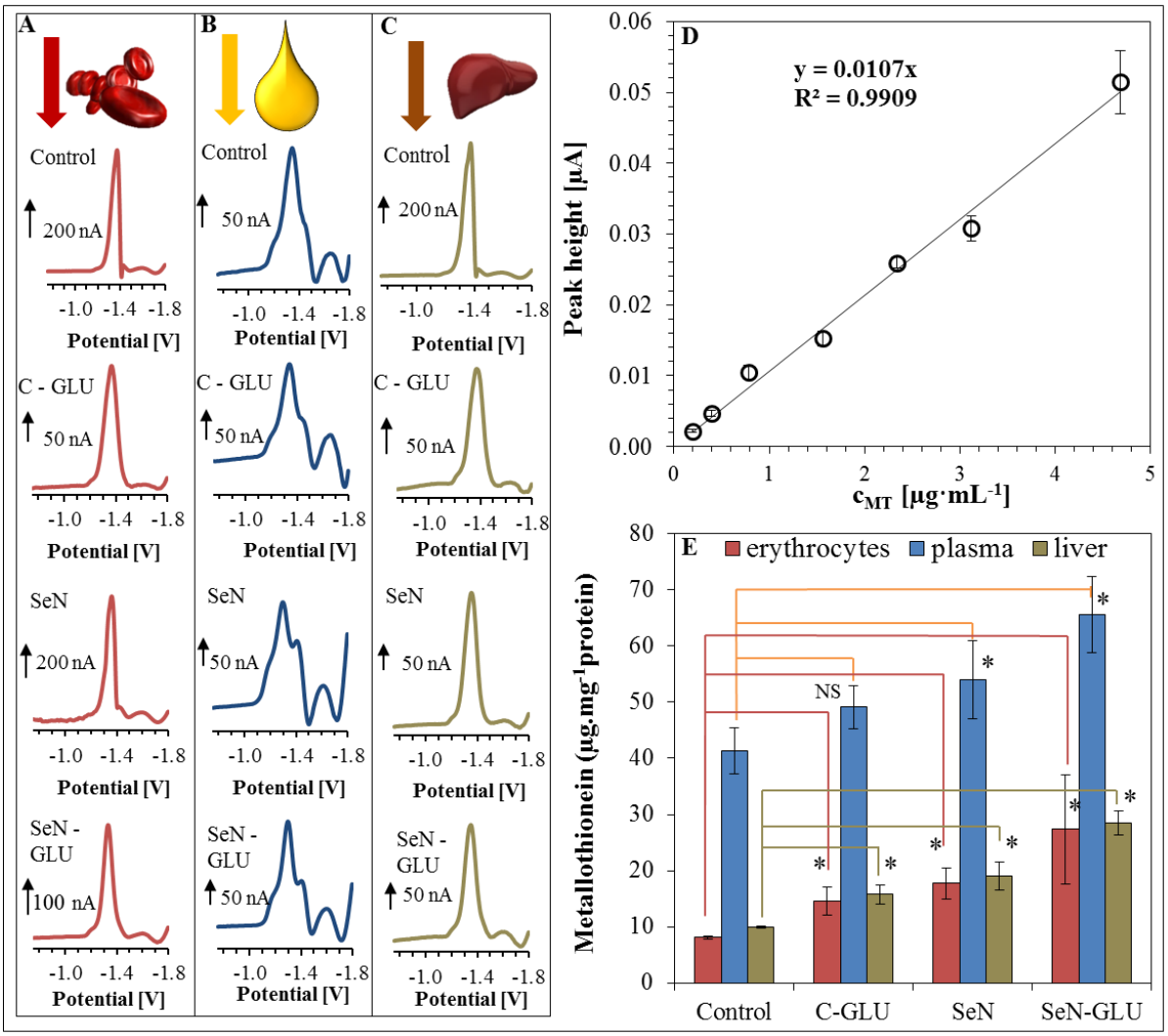

Figure 9. Influence of C-GLU, SeN and SeN-GLU on concentration of MT in **(A)** erythrocytes, **(B)** plasma and **(C)** liver, picture shows a typical voltammograms. **D)** Calibration curve of MT in phosphate buffer (200 mM, pH 7) in concentration range 0.2 – 4.7 µg·mL^{-1}. **E)** Influence of C-GLU, SeN and SeN-GLU on concentration of MT in erythrocytes (red), plasma (blue) and liver (brown) calculated per of mg protein. Data in Fig. 9E represent mean ± s.d. from 5 measurements, NS, not significant, * $P < 0.05$. Other experimental details see in Material and Methods section.

In the evaluation of heavy metals in zinc and copper there were not observed any significant differences between groups in the whole blood or in the liver. Values of zinc in the blood showed a significant decrease in the SeN group by 4% and in the SeN-GLU group by 8%. On the other hand, copper values showed an insignificant increase in the SeN group by 4% and in the SeN-GLU group by 7% (Fig.10A). In the liver samples, an insignificant decrease in zinc values in SeN group by 9% and in SeN-GLU group by 11% was observed. Next, an insignificant decrease in zinc value in SeN group by 9% and SeN-GLU group by 11% was observed (Fig.10 B).

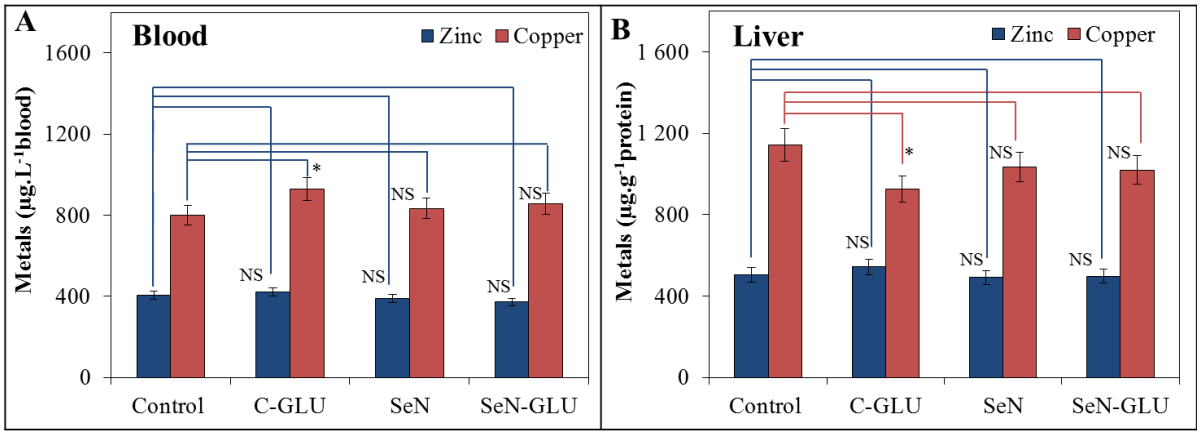

Figure 10. Influence of SeN and SeN-GLU on metal content (zinc and copper) in liver (A) and blood (B). All data represent mean ± s.d. from 5 measurements, NS, not significant, * $P < 0.05$. Other experimental details see in Material and Methods section.

4. DISCUSSION

In the experiment, the influence of an alternative source of selenium (SeN and SeN-GLU) was studied from the viewpoint of its effect on the antioxidative potential of rats. In the similar study, selenium nanoparticles were tested to reduce the effect of radioactive gamma rays. Selenium nanoparticles were fed at a dose of 20 mg per kg of body weight/day and 0.1 mg of Se per kg body weight/day. Selenium nanoparticles were prepared by a different process than we used in our experiment (the average particle size was about 49.6 ± 8.7 nm). Both doses of selenium increased the catalase, glutathione peroxidase (GPx) and superoxide dismutase (SOD) activity in rat blood. The level of selenium and GSH were not affected contrary to our observation [59]. In our experiment, we were able to demonstrate higher levels of GSH in whole blood and plasma in the both SeN a SeN-GLU groups while the levels of GSSG increased less or were lower. Also, the selenium content was higher in the rat blood. We should mention that in our experiment, the rats were not exposed to gamma radiation influencing the antioxidative reaction of the animal organism. Until now, no studies have ever studied the use of nano-dietary selenium and in an experiment, in which the rats were fed with selenium in a dose of 200 µg/kg of body weight (in organic form), the increased GSH content in whole blood of rats was observed after 30 days [60].

In our experiment, an increased activity of GSH and MT has been detected in the SeN and SeN-GLU groups already after 10 days of the experiment. Although, selenium was dosed in a relatively high concentration, the selenium intoxication (probably due to shorter exposition of animals to selenium in the diet) was not observed during the experiment. During study of effect of two different forms of selenium (organic and inorganic) on rats, higher levels of the GPx and SOD antioxidant enzymes were observed in both forms. The amount of malondialdehyde (MDA) [61], which is an indicator of lipid peroxidation, was not affected in any group compared to the control one [62].

Another alternative source of selenium can be *Candida utilis*, which was enriched with selenium, and dosed to rats. This source of selenium increased the antioxidant potential of rats at a dose of 984 μg/kg of diet [63]. In our experiment, increased antioxidant potential, measured by FR, was observed in the groups of SeN a SeN-GLU in the plasma. However, it should be mentioned that the increased antioxidant status was detected in the group, which was dosed with glucose (C-GLU). In our viewpoint, the exposure time (for 10 days) was too short for the exhibition of full effect of selenium. As it is obvious from our results, the erythrocytes well reacted to the selenium addition in the sense of the increasing GSH concentration. Selenium might prove the beneficial effects on the animals exposed to the increased physical stress. In studies according to Akil *et al*., the highest MDA values were detected in the rat group exposed to the physical action. In the erythrocytes, a decrease of GSH, GPx and SOD was observed in the control group. The dose of 6 mg of selenium per kilogram significantly increased GSH, GPx and SOD activities in erythrocytes [64].

In the comparison with our results, it can be stated that the increased antioxidant benefit of selenium in the form of SeN and SeN-GLU was observed in our experiment. The highest levels of GSH, which were used as the antioxidant marker, were detected in the groups of SeN and SeN-GLU. Other studies have demonstrated the effect of selenium (as sodium selenite) on the antioxidant status of the rat livers. Particularly, the influence of selenium on the antioxidant enzymes (especially GPx), occurring in the liver and blood of these animals, was observed. Overall, selenium can have a protective effect on the liver parenchyma, especially in stressful situations [65]. In our observation, the antioxidant enzymes were not the in the centre of our interest.

Because it is an inovative form of selenium, it would be appropriate to carry out further observations and the analysis of the antioxidant enzymes (particularly GPx). Also, the determination of the peroxidation level using the MDA detection can be an interesting experiment. In other studies according to Gabrashanska *et al*., the level of the total antioxidant activity of the organism, measured by the antioxidant enzymes and the rate of peroxidation during dosage of selenium in organic form (as seleno-methionine), was increased. The rats, supplemented with organic selenium, showed higher concentrations of selenium by 19 % in the liver and by 17 % in the plasma in comparison with the control group [66]. In our experiment (although, it was a relatively short selenium exposure for animals), in the whole blood SeN group proved selenium increase by 114 % and SeN-GLU group showed an increase by 52% compared with the control one. According to these results and in comparison with conventional organic source of selenium, selenium particles and selenium particles bounded with glucose proved several times higher usability.

In accordance with the results of other analyzes are also MT levels in erythrocytes, plasma and liver. Generally, the lowest value of the MT has been found in control samples and samples from the C-GLU group. In erythrocyte samples, MT concentrations were the lowest, slightly higher MT concentrations were observed in samples prepared from the liver. The highest concentration (approximately three-fold) were recorded in the case of samples from the collected plasma. C-GLU values were generally higher (20-80%) compared with control values. When SeN group was compared with control, a statistically significant increase in the MT concentrations (120%) in the case of erythrocytes, (31%) in the case of plasma, and (91%) in the case of the liver can be observed. In the case of SeN-GLU group the increase is even more pronounced (258%) in the case of erythrocytes,

(59%) in the case of plasma and (186%) in the case of the liver. Elevated levels of MT together with increased GSH levels indicates antioxidant potential of SeN and SeN-GLU nano-dietary selenium observed in our study.

5. CONCLUSIONS

The experiment, that was focused on the use of dietary selenium nanoparticles and selenium nanoparticles bound with glucose, the positive effect of nanoselenium on the antioxidant status in the body of rats measured by FR, FRAP methods and the GSH and GSSG determination was observed. Both forms of selenium had the effect on the level of reduced and oxidized glutathione in a whole blood and the erythrocytes. Nanoselenium also proved an effect on the amount of metallothionein in the liver and erythrocytes of rats. Furthermore, nano-form of selenium increased the concentration of this element in the blood, liver, and plasma. In case of heavy metals (zinc and copper) determined in liver and blood samples, no significant influence of Se supplementation was observed. The results confirmed that this form of selenium might be used as an alternative source of selenium for the animal organism.

ACKNOWLEDGEMENTS
This project was funded from grants IGA TP 2/2015: Effect of selenium on the quality of plant and animal production from the perspectivy of safety and NAZV QJ1310100 - Development and optimization methods for the determination of biogenic amines in response to increasing health security of silage. Authors thank to Marketa Kominkova and Zuzana Lackova for technical support.

Conflict of interest:
The authors have declared no conflict of interest

References

1. P. Horky, *Ann. Anim. Sci.*, 14 (2014) 869.
2. P. Horky and R. Cerkal, *Potravinarstvo*, 8 (2014) 328.
3. M. Pohanka, B. Ruttkay-Nedecky, J. Fusek, V. Adam and R. Kizek, *Acta Medica,* (Hradec Kralove) 58 (2015) 21.
4. J. Gumulec, M. Raudenska, M. Hlavna, T. Stracina, M. Sztalmachova, V. Tanhauserova, L. Pacal, B. Ruttkay-Nedecky, J. Sochor, O. Zitka, P. Babula, V. Adam, R. Kizek, M. Novakova and M. Masarik, *Exp. Ther. Med.,* 5 (2013) 479.
5. M. Kominkova, P. Horky, N. Cernei, K. Tmejova, B. Ruttkay-Nedecky, R. Guran, M. Pohanka, O. Zitka, V. Adam and R. Kizek, *Int. J. Electrochem. Sci.,* 10 (2015) 1716.
6. P. Herbut, S. Angrecka, G. Nawalany and K. Adamczyk, *Ann. Anim. Sci.,* 15 (2015) 517.
7. P. Horky, K. Tmejova, R. Kensova, N. Cernei, J. Kudr, B. Ruttkay-Nedecky, E. Sapakova, V. Adam and R. Kizek, *Int. J. Electrochem. Sci.,* 10 (2015) 6610.
8. B. Ruttkay-Nedecky, L. Nejdl, J. Gumulec, O. Zitka, M. Masarik, T. Eckschlager, M. Stiborova, V. Adam and R. Kizek, *Int. J. Mol. Sci.,* 14 (2013) 6044.

9. M. Masarik, J. Gumulec, M. Hlavna, M. Sztalmachova, P. Babula, M. Raudenska, M. Pavkova-Goldbergova, N. Cernei, J. Sochor, O. Zitka, B. Ruttkay-Nedecky, S. Krizkova, V. Adam and R. Kizek, *Integr. Biol.*, 4 (2012) 672.
10. R. Brigelius-Flohe and M. Maiorino, *Biochim. Biophys. Acta-Gen. Subj.*, 1830 (2013) 3289.
11. P. Horky, P. Jancikova, J. Sochor, D. Hynek, G. J. Chavis, B. Ruttkay-Nedecky, N. Cernei, O. Zitka, L. Zeman, V. Adam and R. Kizek, *Int. J. Electrochem. Sci.*, 7 (2012) 9643.
12. P. Horky, Ann. *Anim. Sci.*, 14 (2014) 341.
13. P. Herbut and S. Angrecka, *Ann. Anim. Sci.*, 14 (2014) 153.
14. P. Horky, P. Jancikova and L. Zeman, *Acta Univ. agric. Silvic. Mendel. Brun.*, 60 (2012) 49.
15. P. Nevrkla, M. Cechova and Z. Hadas, *Acta Vet.*, BRNO 83 (2014) 321.
16. P. Horky, B. Ruttkay-Nedecky, M. Kremplova, O. Krystofova, R. Kensova, D. Hynek, P. Babula, O. Zitka, L. Zeman, V. Adam and R. Kizek, *Int. J. Electrochem. Sci.*, 8 (2013) 6162.
17. S. Ashouri, S. Keyvanshokooh, A. P. Salati, S. A. Johari and H. Pasha-Zanoosi, *Aquaculture*, 446 (2015) 25.
18. J. Sochor, M. Pohanka, B. Ruttkay-Nedecky, O. Zitka, D. Hynek, P. Mares, L. Zeman, V. Adam and R. Kizek, *Cent. Eur. J. Chem.*, 10 (2012) 1442.
19. L. C. Clark, B. Dalkin, A. Krongrad, G. F. Combs, B. W. Turnbull, E. H. Slate, R. Witherington, J. H. Herlong, E. Janosko, D. Carpenter, C. Borosso, S. Falk and J. Rounder, *Br. J. Urol.*, 81 (1998) 730.
20. M. P. Rayman, *Proc. Nutr. Soc.*, 64 (2005) 527.
21. J. J. Yang, K. H. Huang, S. Y. Qin, X. S. Wu, Z. P. Zhao and F. Chen, *Dig. Dis. Sci.*, 54 (2009) 246.
22. X. X. Zhou, Y. B. Wang, Q. Gu and W. F. Li, *Aquaculture*, 291 (2009) 78.
23. S. Karamipour, M. S. Sadjadi and N. Farhadyar, *Spectroc. Acta Pt. A-Molec. Biomolec. Spectr.*, 148 (2015) 146.
24. P. A. Tran and T. J. Webster, *Int. J. Nanomed.*, 6 (2011) 1553.
25. J. S. Zhang, X. Y. Gao, L. D. Zhang and Y. P. Bao, *Biofactors*, 15 (2001) 27.
26. H. L. Wang, J. S. Zhang and H. Q. Yu, Free Radic. *Biol. Med.*, 42 (2007) 1524.
27. J. S. Zhang, X. F. Wang and T. W. Xu, *Toxicol. Sci.*, 101 (2008) 22.
28. D. G. Peng, J. S. Zhang, Q. L. Liu and E. W. Taylor, *J. Inorg. Biochem.*, 101 (2007) 1457.
29. B. Huang, J. S. Zhang, J. W. Hou and C. Chen, *Free Radic. Biol. Med.*, 35 (2003) 805.
30. J. Sochor, J. Dobes, O. Krystofova, B. Ruttkay-Nedecky, P. Babula, M. Pohanka, T. Jurikova, O. Zitka, V. Adam, B. Klejdus and R. Kizek, *Int. J. Electrochem. Sci.*, 8 (2013) 8464.
31. L. Nejdl, J. Sochor, O. Zitka, N. Cernei, B. Ruttkay-Nedecky, P. Kopel, P. Babula, V. Adam, J. Hubalek and R. Kizek, *Chromatographia*, 76 (2013) 363.
32. M. Pohanka, D. Hynek, A. Kracmarova, J. Kruseova, B. Ruttkay-Nedecky, J. Sochor, V. Adam, J. Hubalek, M. Masarik, T. Eckschlager and R. Kizek, *Int. J. Electrochem. Sci.*, 7 (2012) 11978.
33. D. Hynek, J. Prasek, P. Businova, J. Zak, J. Drbohlavova, J. Chomoucka, J. Kynicky, M. Konecna, M. Brnicky, J. Hubalek, R. Vrba, R. Kizek and V. Adam, *Int. J. Electrochem. Sci.*, 8 (2013) 4441.
34. J. Prasek, L. Trnkova, I. Gablech, P. Businova, J. Drbohlavova, J. Chomoucka, V. Adam, R. Kizek and J. Hubalek, *Int. J. Electrochem. Sci.*, 7 (2012) 1785.
35. O. Zitka, D. Huska, V. Adam, A. Horna, J. Hubalek, M. Beklova and R. Kizek, *Toxicol. Lett.*, 189 (2009) S126.
36. O. Zitka, K. Stejskal, A. Kleckerova, V. Adam, M. Beklova, A. Horna, V. Supalkova, L. Havel and R. Kizek, *Chem. Listy*, 101 (2007) 225.
37. J. Dobes, O. Zitka, J. Sochor, B. Ruttkay-Nedecky, P. Babula, M. Beklova, J. Kynicky, J. Hubalek, B. Klejdus, R. Kizek and V. Adam, *Int. J. Electrochem. Sci.*, 8 (2013) 4520.

38. O. Zitka, S. Skalickova, J. Gumulec, M. Masarik, V. Adam, J. Hubalek, L. Trnkova, J. Kruseova, T. Eckschlager and R. Kizek, *Oncol. Lett.*, 4 (2012) 1247.
39. J. Sochor, P. Babula, B. Krska, A. Horna, I. Provaznik, J. Hubalek and R. Kizek, in J. Jan, R. Jirik, R. Kolar, J. Kolarova, J. Kozumplik, I. Provaznik (Editors), Analysis of Biomedical Signals and Images, Brno Univ Technology Vut Press, Brno (2010).
40. O. Zitka, S. Krizkova, S. Skalickova, P. Kopel, P. Babula, V. Adam and R. Kizek, Comb. *Chem. High Throughput Screen*, 16 (2013) 130.
41. V. Diopan, V. Shestivska, O. Zitka, M. Galiova, V. Adam, J. Kaiser, A. Horna, K. Novotny, M. Liska, L. Havel, J. Zehnalek and R. Kizek, *Electroanalysis*, 22 (2010) 1248.
42. J. Petrlova, R. Mikelova, K. Stejskal, A. Kleckerova, O. Zitka, J. Petrek, L. Havel, J. Zehnalek, V. Adam, L. Trnkova and R. Kizek, *J. Sep. Sci.*, 29 (2006) 1166.
43. D. Chudobova, K. Cihalova, S. Dostalova, B. Ruttkay-Nedecky, M. A. M. Rodrigo, K. Tmejova, P. Kopel, L. Nejdl, J. Kudr, J. Gumulec, S. Krizkova, J. Kynicky, R. Kizek and V. Adam, *FEMS Microbiol. Lett.*, 351 (2014) 195.
44. D. Potesil, J. Petrlova, V. Adam, J. Vacek, B. Klejdus, J. Zehnalek, L. Trnkova, L. Havel and R. Kizek, *J Chromatogr. A*, 1084 (2005) 134.
45. J. Petrlova, R. Mikelova, K. Stejskal, A. Kleckerova, O. Zitka, J. Petrek, L. Havel, J. Zehnalek, V. Adam, L. Trnkova and R. Kizek, *J. Sep. Sci.*, 29 (2006) 1166.
46. K. Stejskal, Z. Svobodova, I. Fabrik, V. Adam, M. Beklova, M. Rodina and R. Kizek, *J Appl Ichthyol*, 24 (2008) 519.
47. V. Diopan, K. Stejskal, M. Galiova, V. Adam, J. Kaiser, A. Horna, K. Novotny, M. Liska, L. Havel, J. Zehnalek and R. Kizek, *Electroanalysis*, 22 (2010) 1248.
48. M. Pohanka, J. Sochor, B. Ruttkay-Nedecky, N. Cernei, V. Adam, J. Hubalek, M. Stiborova, T. Eckschlager and R. Kizek, *J. Appl. Biomed.*,10 (2012) 155.
49. J. Petrlova, D. Potesil, R. Mikelova, O. Blastik, V. Adam, L. Trnkova, F. Jelen, R. Prusa, J. Kukacka and R. Kizek, *Electrochim. Acta*, 51 (2006) 5112.
50. I. Fabrik, S. Krizkova, D. Huska, V. Adam, J. Hubalek, L. Trnkova, T. Eckschlager, J. Kukacka, R. Prusa and R. Kizek, *Electroanalysis*, 20 (2008) 1521.
51. L. Krejcova, I. Fabrik, D. Hynek, S. Krizkova, J. Gumulec, M. Ryvolova, V. Adam, P. Babula, L. Trnkova, M. Stiborova, J. Hubalek, M. Masarik, H. Binkova, T. Eckschlager and R. Kizek, *Int. J. Electrochem. Sci*., 7 (2012) 1767.
52. J. Sochor, D. Hynek, L. Krejcova, I. Fabrik, S. Krizkova, J. Gumulec, V. Adam, P. Babula, L. Trnkova, M. Stiborova, J. Hubalek, M. Masarik, H. Binkova, T. Eckschlager and R. Kizek, *In.t J. Electrochem. Sci.*, 7 (2012) 2136.
53. G. L. Long and J. D. Winefordner, *Anal. Chem.*. 55 (1983) A712.
54. P. Cartes, L. Gianfreda and M. L. Mora, *Plant Soil*, 276 (2005) 359.
55. M. Kominkova, R. Guran, M. A. M. Rodrigo, P. Kopel, I. Blazkova, D. Chudobova, L. Nejdl, Z. Heger, B. Ruttkay-Nedecky, O. Zitka, V. Adam and R. Kizek, *Int. J. Electrochem. Sci*., 9 (2014) 2993.
56. N. Cernei, Z. Heger, P. Kopel, V. Milosavljevic, M. Kominkova, A. Moulick, O. Zitka, L. Trnkova, V. Adam and R. Kizek, *Int. J. Electrochem. Sci.*, 9 (2014) 3386.
57. O. Zitka, M. Kominkova, S. Skalickova, H. Skutkova, I. Provaznik, T. Eckschlager, M. Stiborova, V. Adam, L. Trnkova and R. Kizek, *Int. J Electrochem. Sci*,. 7 (2012) 10544.
58. K. M. Anjum, M. S. Mughal, U. Sayyed, A. Yaqub, A. Khalique, M. A. Rashid, M. Z. Yousaf and N. Mumtaz, *J. Anim. Plant. Sci.*, 24 (2014) 77.
59. A. I. El-Batal, N. M. Thabet, A. O. Mostafa, A. R. B. Abdel Ghaffar and K. S. Azab, *World Appl. Sci. J.*, 19 (2012) 962.
60. F. M. El-Demerdash and H. M. Nasr, *J. Trace Elem. Med. Bio.*, 28 (2014) 89.
61. S. Rakshit, B. S. Chandrasekar, B. Saha, E. S. Victor, S. Majumdar and D. Nandi, *Biochim. Biophys. Acta*, 1843 (2014) 2645.

62. I. Musik, M. Kielczykowska and J. Kocot, *Bul.l Vet. Inst. Pulawy*, 57 (2013) 449.
63. B. Yang, D. Wang, G. Wei, Z. Liu and X. Ge, *J. Trace Elem. Med. Bio.*, 27 (2013) 7.
64. M. Akil, U. Gurbuz, M. Bicer, A. Sivrikaya, R. Mogulkoc and A. K. Baltaci, *Biol. Trace Elem. Res.*, 142 (2011) 651.
65. S. Ghodbane, S. Amara, C. Garrel, J. Arnaud, V. Ducros, A. Favier, M. Sakly and H. Abdelmelek, *Environ. Toxicol. Phar.*, 31 (2011) 100.
66. M. Gabrashanska, S. E. Teodorova, S. Petkova, L. Mihov, M. Anisimova and D. Ivanov, *Parasitol. Res*., 106 (2010) 561.